Intracluster Electron Transfer and Reactions in Alkali Metal−Methacrylate Clusters

Hironori Tsunoyama, Keijiro Ohshimo, Fuminori Misaizu,*,† and Koichi Ohno*,‡

Department of Chemistry, Graduate School of Science, Tohoku University, Aramaki, Aoba-ku, Sendai 980-8578, Japan

Received: May 16, 2001; In Final Form: August 7, 2001

Size-dependent stability and intracluster reactions have been investigated by photoionization mass spectrometry for alkali metal (M = Li, Na, and K)−methacrylate (CH_2═$C(CH_3)CO_2R$; R═CH_3 and C_2H_5) clusters. The following two features are commonly observed in the mass spectra of $M(CH_2$═$C(CH_3)CO_2R)_n$ clusters; (1) enhanced ion signal (magic number) at $n = 3$, and (2) fragment ions with a loss of ROH only for $n = 3$ and 2. In addition, the magic number behavior at $n = 6$ is also observed in K system. These features are explained by an intracluster oligomerization and following dissociation reactions. The magic number trimer has a cyclohexane structure as a result of oligomerization, and the two dissociative products also have cyclic structures. The loss of ROH from $n = 3$ and $n = 2$ cluster can be attributed to Dieckmann cyclization and lactonization reaction, respectively. From the size-dependent additivity of H_2O to M(methacrylate)$_n$ clusters, the numbers of methacrylate molecules filling the first solvation shell for Li, Na, and K systems are estimated to be 4, 5, and 6, respectively. From the consideration of the intracluster oligomerization, it is suggested that one and two methacrylate molecules directly bind to the metal atom in Li and Na systems, respectively, in addition to one cyclohexane derivatives. In the K system, two cyclohexanes are suggested to bind directly to the K atom, which is consistent with the observation of the $n = 6$ magic number.

1. Introduction

Much attention has been paid for anionic polymerization of vinyl compounds for several decades as a method to obtain various useful materials.[1,2] In the condensed phase, it is well-known that strong bases initiate anionic polymerization of vinyl compounds which have electron withdrawing substituents, such as cyano (−CN) and carboxyl ($-CO_2R$) groups. Alkali metals and alkyllithium compounds are used as strong bases to initiate such polymerization reaction. Anionic polymerization reaction is known to be composed of the following three steps. Electron transfer from the base species causes cleavage of the C═C double bond of a monomer and yields a corresponding carbanion (initiation step). This carbanion reacts with other monomers successively and yields propagated carbanion (propagation step). Finally, electron transfer from carbanion to counterion or the reaction which produces an unreactive isomeric carbanion terminates the polymerization reaction (termination step).

Despite extensive studies of the anionic polymerization reaction and its wide application, details of the elementary reaction processes especially in the early stage of anionic polymerization have not been well elucidated. For this purpose, anionic oligomerization in the gas phase,[3−15] as well as cationic oligomerization,[16−27] have been studied. These gas-phase studies have some advantages: (1) it is possible to discuss reactivity in detail in simple systems which are free from solvent effects, and (2) assignments of reaction products can be made directly on the basis of mass spectrometric method. Models for the initiation step of anionic polymerization in the gas phase can be classified into two types in terms of the environments of reactant species; (1) a free anion of a vinyl molecule solvated with other vinyl monomers, and (2) an ion-pair formed between a base and vinyl monomers.

McDonald and Chowdhury investigated the gas-phase anionic oligomerization of methyl acrylate (MA; CH_2═$CHCO_2CH_3$) initiated by molecular negative ions, such as F_3C^-, $NCCH_2^-$, and $C_3H_5^-$, in a flowing afterglow apparatus.[3] This study is based on a free anion model noted above. They found that oligomerization terminates at the trimer, irrespective of the reaction initiator in gas-phase ion−molecule reactions. They concluded that this termination should be attributed to the following two reactions; (1) Dieckmann cyclization followed by a loss of CH_3OH to form an unreactive conjugate base of cyclized β-ketoester, and (2) intramolecular H^+ transfer to produce an isomeric unreactive enolate anion. As another approach of anionic oligomerization with the free anion model, gas-phase studies on cluster anions were performed.[5−12] Tsukuda, Kondow, and their co-workers have extensively investigated cluster anions of various vinyl compounds produced by electron transfer from high-Rydberg rare gas atoms.[5−7] In the anion clusters of acrylonitrile (AN; CH_2═$CHCN$) and its derivatives, the magic number behavior at $n = 3k$ was observed in the mass spectra. From detailed studies using photodissociation,[8] photoelectron,[9,10] and collision-induced dissociation,[11] the magic number behavior was attributed to trimeric termination of oligomerization by cyclization producing stable cyclohexane derivatives. On the other hand, no pronounced signals at $n = 3$ were observed in the mass spectrum of MA and methyl methacrylate (MMA) cluster anions, $(MA)_n^-$ and $(MMA)_n^-$.[5]

Clusters containing neutral initiator species and vinyl molecules, which is regarded as a contact ion pair model, were investigated by the authors in order to discuss the mechanism of the propagation steps of the ion pair with another monomer.[13−15] Intracluster reactions have been investigated for clusters containing an alkali atom and vinyl molecules by means of a time-

* Corresponding authors.
† E-mail: misaizu@qpcrkk.chem. tohoku.ac.jp.
‡ E-mail: ohnok@qpcrkk.chem.tohoku.ac.jp.

10.1021/jp0118930 CCC: $20.00
Published on Web 10/03/2001

of-flight (TOF) mass spectrometry coupled with a laser photoionization. In clusters of a neutral alkali atom M (M = Li, Na, and K) with AN molecules, $M(AN)_n$, the magic numbers at $n = 3k$ ($k = 1-4$) were observed in the photoionization mass spectra.[13,14] It should be noted that the trimeric unit with a cyclohexane ring is produced by anionic oligomerization initiated by electron transfer from an alkali atom. In the case of acrylic ester and alkali atom clusters, the same magic number behavior at $n = 3$ was observed in the mass spectra.[15] In addition, the fragmented cluster ions with a loss of alcohol were detected only for $n = 3$. This fragmentation reaction was explained by Dieckmann cyclization after anionic oligomerization to produce another isomer of the trimer followed by electron transfer from the metal atom. In the $M(acrylate)_3$ cluster, it is expected that the trimeric cyclization reaction competes with Dieckmann cyclization. In these intracluster reactions, electron density at the α carbon (carbon atom with a carboxyl group) is important because these two competitive reactions are nucleophilic addition by the α carbon. Therefore, an introduction of another substituent to the α carbon is expected to change the reaction ratio between these two reactions.

In the present paper, we have investigated clusters containing an alkali metal atom (M = Li, Na, and K) and methacrylic ester molecules [$CH_2{=}C(CH_3)CO_2R$ ($R{=}CH_3$ and C_2H_5)] by photoionization mass spectrometry. Methacrylic ester has a structure in which methyl group introduced to the α carbon of acrylic ester. The intracluster oligomerization reaction caused by electron transfer from the metal atom to molecules is discussed from the size distributions observed in the mass spectra. We have also measured the photoionization mass spectra of alkali metal−MMA−H_2O clusters. The structures of $M(MMA)_n$ clusters are discussed from the size-dependent additivity of H_2O to $M(MMA)_n$ clusters. Quantum chemical calculation based on density functional theory (DFT) was performed in order to obtain further insight into the intracluster reaction initiated by the alkali atom and geometrical structures of the products.

2. Experimental Section

Details of the experimental setup have been described in previous publications.[13−15] Briefly, the system is composed of two-stage differentially evacuated chambers which contain a cluster beam source and a Wiley−McLaren type time-of-flight mass spectrometer (TOF-MS).[28] Clusters of alkali metal and methacrylic ester molecules, $M(CH_2{=}C(CH_3)CO_2R)$ (M = Li, Na, and K; $R{=}CH_3$ and C_2H_5), were generated by a pickup source.[29−31] The methacrylic ester vapor mixed with He in a sample reservoir was expanded from a pulsed valve with a total pressure of 4 atm. Metal vapor was generated by irradiation with the second harmonic of a Nd:YAG laser (Lumonics, HY-400) to a metal rod placed at a distance of 10 mm from the nozzle exit of the valve. The vaporized metal atoms immediately collide and react with molecular clusters formed in the pulsed jet. The neutral species were introduced to the TOF-MS chamber after collimation with a conical skimmer. A dye laser (Spectra-Physics, PDL-2) pumped by a Nd:YAG laser (Spectra-Physics, GCR-150-10), along with a second harmonic generator (Inrad, Autotracker III), was used as the ionization light source. We kept the fluence of the ionization laser under 4 mJ cm^{-2} during measurement in order to avoid multiphoton ionization processes. The cluster ions formed by one-photon ionization were accelerated by static electric fields to ∼3.0 keV and were introduced into a 550-mm field-free tube. The mass-separated ions were detected by a dual-microchannel plate (Hamamatsu, F1552-21S) at the end of the flight tube, and output signals were stored by a digital oscilloscope (LeCroy, 9344C).

For the preparation of M−MMA−H_2O clusters, we used two sample reservoirs containing MMA and H_2O, respectively, with serial connection. The mixing ratio of H_2O:MMA:He was changed by an independent temperature control of each sample reservoirs. The mixed gas of MMA, H_2O, and He was expanded from the pulsed valve with a stagnation pressure of 4 atm. The molecular clusters collide and react with vaporized metal atoms produced by laser vaporization. The resultant neutral species were ionized and detected as noted above.

The sample rods of sodium and potassium were made from a lump under a nitrogen atmosphere in a vacuum-drybox to avoid the reaction with water in the air. The lithium rod was made in the same way under argon atmosphere in order to avoid the reactions with nitrogen and water. Chemicals were purchased at the following minimum percent impurities and used without further purification: MMA (Nacalai, 99%), ethyl methacrylate (EMA) (Wako, 99%).

3. Calculation

We performed quantum chemical calculations for free MMA and Na(MMA) to examine the possibility of electron transfer. All calculations were carried out by using a DFT program of the Gaussian94 package.[32] The 6-31+G(d) basis set and B3LYP functional[33] were utilized in these calculations. For a free MMA molecule, two conformational isomers, *s-cis* and *s-trans*, were estimated to be in equilibrium with a relative abundance of *s-cis*: *s-trans* = 36:64 at room temperature.[34] Therefore, we employed a geometrical optimization of MMA and Na(MMA) for two isomers. The calculated bond length and bond angles of *s-trans* MMA showed excellent agreement (within 0.01 Å and 0.1 degree) with those of experimental data obtained by electron diffraction technique.[34] The electron density distribution of Na(MMA) was also calculated to discuss the intracluster electron transfer. For the discussion about the contribution of each isomer to the reaction with the metal, we also calculated the potential energy curve for C−C rotation of free MMA and estimated the rotational barrier for *s-trans* to *s-cis* conformational change at B3LYP/6-31+G(d) level. To discuss the structure of intracluster oligomerization product, we also performed geometrical optimization of trimethyl 1,3,5-trimethylcyclohexane-1,3,5-tricarboxylate (TMTMCHTCX) at the HF/6-31G level.

4. Results and Discussion

A. The Size Distributions in the Photoionization Mass Spectra of $M(EMA)_n$ and $M(MMA)_n$ (M = Na, K, and Li). Typical photoionization mass spectra of $Na(EMA)_n$ and $Na(MMA)_n$ obtained by 5.64-eV laser irradiation are shown in Figure 1. In this figure, the cluster ion series of $Na^+(EMA)_n$ and $Na^+(MMA)_n$ are predominant. In addition, $Na^+(EMA)_n(H_2O)_m$ and $Na^+(MMA)_n(H_2O)_m$ cluster ion series are also detected as side peaks at $n \geq 6$ clusters. These hydrated ions are due to water impurity in methacrylate sample. In the mass spectrum of Na−MMA−H_2O system, this feature is also observed at higher water mixing ratio (see Section 4E). Furthermore, fragment ion peaks denoted by arrows with circles in Figure 1 are also found in both systems. These fragment species are assigned to be a loss of ROH from the $n = 2$ and 3 clusters. We also measured the photoionization mass spectra of K−methacrylate clusters (Figure 2) and Li−methacrylate clusters (Figure 3). In Figure 2, $K^+(EMA)_n$ and $K^+(MMA)_n$ ion series are predominant with several side peaks assignable to $[K(methacrylate)_nKOH]^+$ which contain KOH impurity in K rod. Fragment ion peaks denoted by arrows with circles are assignable to the loss of ROH from $n = 2$ and 3. In addition,

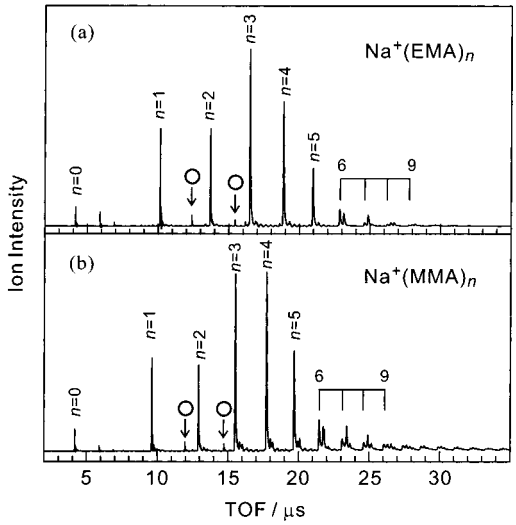

Figure 1. Typical photoionization mass spectra of (a) Na(EMA)$_n$ and (b) Na(MMA)$_n$ obtained by one-photon ionization of 5.64 eV. Series of cluster ions $Na^+(EMA)_n$ and $Na^+(MMA)_n$ are predominantly observed. In both mass spectra, peaks denoted by arrows with circles are also assignable to a loss of (a) C_2H_5OH and (b) CH_3OH from $n = 2$ and 3 for Na−EMA and Na−MMA systems, respectively. Small side peaks with $n \geq 6$ clusters are assignable to $Na^+(EMA)_n(H_2O)_m$ and $Na^+(MMA)_n(H_2O)_m$ for (a) and (b), respectively.

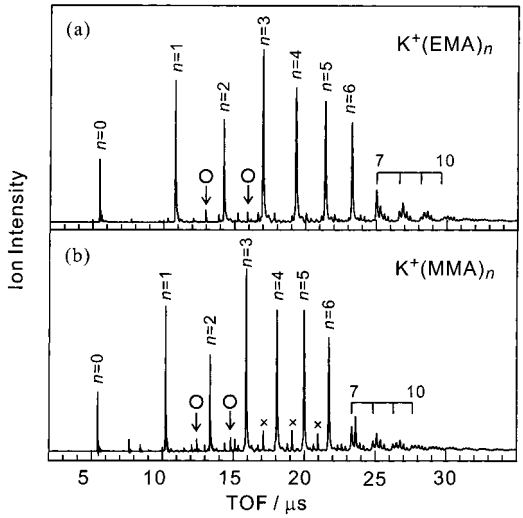

Figure 2. Typical photoionization mass spectra of (a) K(EMA)$_n$ and (b) K(MMA)$_n$. The photon energy was 5.64 eV. Series of $K^+(EMA)_n$ and $K^+(MMA)_n$ are predominantly observed. Several side peaks denoted by × between $n = 3$ and 6 are assignable to $K^+(MMA)_nKOH$ caused by KOH impurity of K rod. In both mass spectra, peaks denoted by arrows with circles are also assignable to a loss of (a) C_2H_5OH and (b) CH_3OH from $n = 2$ and 3 for K−EMA and K−MMA systems, respectively. Small side peaks with $n \geq 7$ clusters are assignable to $K^+(EMA)_n(H_2O)_m$ and $K^+(MMA)_n(H_2O)_m$ for (a) and (b), respectively.

$K^+(EMA)_n(H_2O)_m$ and $K^+(MMA)_n(H_2O)_m$ cluster ion series are also detected as side peaks at $n \geq 7$ clusters. In Figure 3, $Li^+(EMA)_n$ and $Li^+(MMA)_n$ ion series are predominant with the fragment ions denoted by arrows with circles as well as Na and K cases. In these experiments, one-photon ionization is expected to take place, because alkali atoms have low ionization energies (5.39, 5.14, and 4.34 eV for Li, Na, and K, respectively). Therefore, only the clusters containing alkali atom are detected in the mass spectra. In all mass spectra (Figures 1−3), the intensity enhancement (magic number) at $n = 3$ is commonly found; the intensities at $n = 3$ are at least two times larger than those at $n = 2$. In addition, ions for $n = 4$ and 5 are strongly

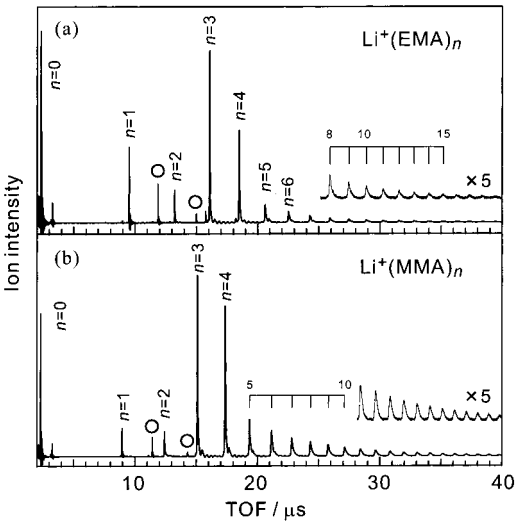

Figure 3. Typical photoionization mass spectra of (a) Li(EMA)$_n$ and (b) Li(MMA)$_n$ obtained by one-photon ionization of 5.64 eV. Series of cluster ions $Li^+(EMA)_n$ and $Li^+(MMA)_n$ are predominantly observed. In both mass spectra, peaks denoted by arrows with circles are also assignable to a loss of (a) C_2H_5OH and (b) CH_3OH from $n = 2$ and 3 for Li-EMA and Li-MMA systems, respectively.

observed depending on the alkali metal atom. Also the large intensity difference between $n = 6$ and 7 cluster is observed only in the K−methacrylate systems. Thus the $n = 6$ cluster is also considered to be a magic number in these systems. As another common feature, the peaks caused by the loss of CH_3OH or C_2H_5OH are detected only from $n = 2$ and 3 ions. These features are independent of the ionization laser wavelength between 4.66 and 5.64 eV.

B. Origin of the Appearance of the Magic Number Behavior. In our cluster source, the metal atom−methacrylate clusters are produced by the collision of the vaporized metal atom with molecular clusters preformed by supersonic expansion along with the collisional cooling by He buffer gas. In this source, cluster ions can also be produced directly by laser vaporization followed by metal ion−molecule reactions. In the mass spectra of these nascently produced K−methacrylate cluster ions, no intensity enhancements as in Figure 2 are observed.[35] Therefore the magic number behavior observed in the photoionization of the neutral clusters originates from the following three possibilities: (1) stable complex formation between neutral alkali atom and methacrylate clusters, (2) size-dependent ionization efficiency of M−methacrylate clusters, and (3) size-dependent numbers of evaporated molecules after ionization. Among these, (2) and (3) are safely ruled out as thoroughly discussed in the acrylate case, [15] because the magic number behavior is found to be independent of the ionization laser wavelength between 4.66 and 5.64 eV. Therefore, (1) is most probable; the magic numbers can be related to the nature of neutral alkali atom−methacrylate clusters.

Clusters in the present study are considered to be a model of the portion of anionic polymerization in bulk solution. AN anion clusters,[6] alkali atom−AN clusters,[13,14] and alkali atom−acrylate clusters[15] were studied by means of a mass spectrometry, and the same magic numbers at $n = 3$ were observed in their mass spectra. In those papers, the magic numbers at $n = 3$ were attributed to the formation of cyclohexane derivatives by intracluster anionic oligomerization. In bulk solution, the reactivity of methacrylate for anionic polymerization is known to be comparable with that of acrylate. Therefore, the same reaction as the metal−acrylate system is expected to proceed

SCHEME 1

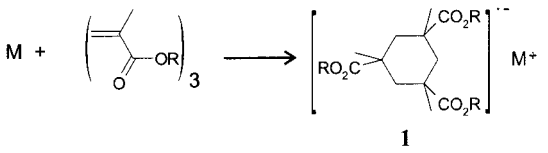

1

in the present metal−methacrylate system. We concluded that the magic number at $n = 3$ originates from forming a cyclohexane derivative (trimethyl 1,3,5-trimethylcyclohexane-1,3,5-tricarboxylate, TMTMCHTCX) by intracluster anionic oligomerization (Scheme 1).

In the photoionization mass spectra of $M(MMA)_n$ and $M(EMA)_n$, $n = 4$ cluster ions have comparable intensities with $n = 3$. The clusters for $n = 4$ and 5 are expected to contain one cyclohexane derivative and one and two monomer(s), respectively. This involvement of a cyclohexane derivative for $n > 3$ clusters is supported by photodissociation of neutral clusters[14] and also by negative-ion photoelectron spectroscopy[36] of metal−AN clusters, although the ions for $n = 4$ and 5 were neither strongly observed in those systems[13,14] nor in metal−acrylate clusters.[15] As discussed in the previous papers,[13−15] the appearance of the magic number behavior is expected to be a result of evaporation processes after intracluster reaction. Thus the intensity enhancement at $n = 4$ and 5 in the present metal−methacrylate clusters indicates the suppression of evaporation of monomers. In other words, the binding energies of the unreacted methacrylate monomer in the present clusters are presumed to be larger than those in other metal−vinyl molecules systems, although no qualitative information is available at present. In addition, a magic number at $n = 6$ is observed in the mass spectra of K−methacrylate system. This feature was also observed in metal−acrylate system, so that this magic number is ascribable to two successive cyclization reactions to form two cyclohexane units. However, the magic number behavior at $n = 6$ was not remarkably observed in Li and Na systems. The intracluster oligomerization in metal−vinyl molecules clusters is induced by electron transfer from the alkali metal atom to monomers. Thus the electron which induces the first cyclization reaction is expected to have an important role also in the second cyclization; the second cyclization reaction is induced by transfer of the electron which induces the first reaction. This second electron transfer has a possibility to occur through the metal atom (ion) after returning of the electron from the first cyclized product, on the basis of the termination reaction of the anionic polymerization in bulk solution.[37] Therefore, the direct interactions between the metal atom and the methacrylate monomers are presumed to be important for the second electron transfer, and thus, for the second cyclization reaction. The number of monomers that directly interact with the metal atom is probably more than 6 in K systems, whereas the numbers are restricted to be smaller than 6 for Li and Na systems by their small atomic radii, as discussed in Section 4E. As a result, the second cyclization reaction is expected to be inhibited for the latter two metal systems.

C. Calculated Structures of Na(MMA) and the Possibility of Intracluster Electron Transfer. To get further insight into the intracluster electron transfer, we have optimized the structure of Na(MMA) based on DFT (B3LYP/6-31+G(d)). As noted in Section 3, a free MMA molecule has two conformational isomers, *s-cis* and *s-trans*, with a relative abundance of *s-cis*: *s-trans* = 36:64 at room temperature.[34] From the geometrical optimizations of two isomers for free MMA, the *s-trans* isomer is 0.21 kcal/mol more stable than *s-cis* isomer. The rotational

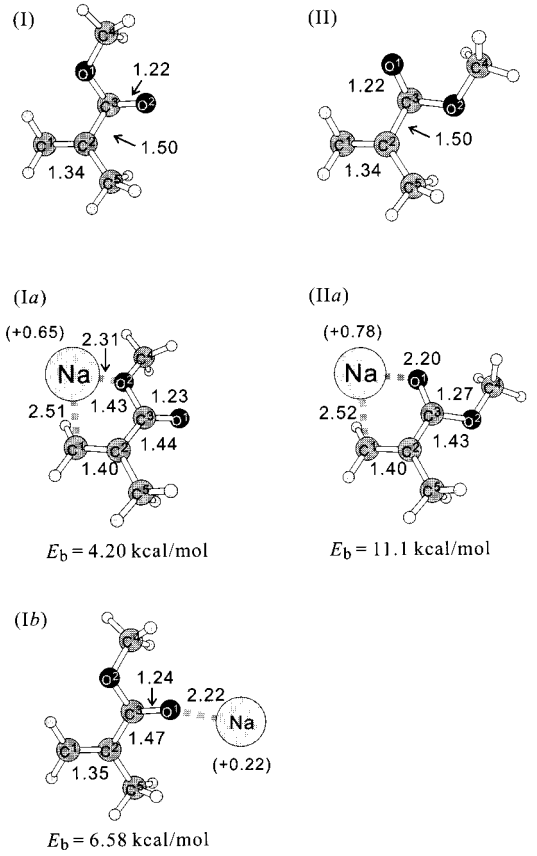

Figure 4. Optimized structures of free (I) *s-trans* MMA and (II) *s-cis* MMA calculated by B3LYP/6-31+G(d) level. Energy difference between these isomers is estimated to be 0.21 kcal/mol. Optimized neutral Na(*s-trans* MMA) complex (I*a* and I*b*) and (*s-cis* MMA) complex (II*a*) are also shown. Bond lengths and angles are shown in Å and degrees, respectively. Binding energy between Na and corresponding MMA isomer (E_b) in each complex is also shown. Values in parentheses are natural charges on a Na atom.

barrier of the C^2-C^3 bond from the *s-trans* isomer in the free MMA molecule is estimated to be 5.1 kcal/mol at the B3LYP/6-31+G(d) level. For the Na(*s-trans* MMA) complex, we performed geometrical optimization and found two stable structures. The optimized structures of Na(*s-trans* MMA) along with the binding energies are shown in Figure 4(I). In both structures I*a* and I*b*, the valence electron of Na is found to transfer into MMA to some extent; the natural charge on Na in each complex is +0.65 (for I*a*) and +0.22 (for I*b*), respectively. We also optimized the structure of Na(*s-cis* MMA) and found one equilibrium structure II*a* shown in Figure 4(II). The binding energy in isomer II*a* is larger than those in other two isomers, and II*a* is the most stable structure. Isomer II*a* has a possibility to be produced in the cluster source, because the rotational barrier of C^2-C^3 is smaller than the binding energy of M−MMA in I*b*. In contrast, isomerization from I*a* to II*a* is less possible, because the counterion binds to oxygen of $-OCH_3$ and restricts the conformational change. However, in our experimental setup, an alkali metal atom with high kinetic energy collides with methacrylate cluster formed by the pulsed jet under the collisional cooling condition, so that $M(MMA)_n$ clusters are formed at high-temperature condition. Therefore, the structural change among isomers may be possible at the present condition.

In the most stable structure II*a*, the $C^1=C^2$ and $C^3=O^1$ bond lengths are ∼5% longer than those of the free MMA molecule. In contrast, the bond length of C^2-C^3 is ∼5% shorter. These

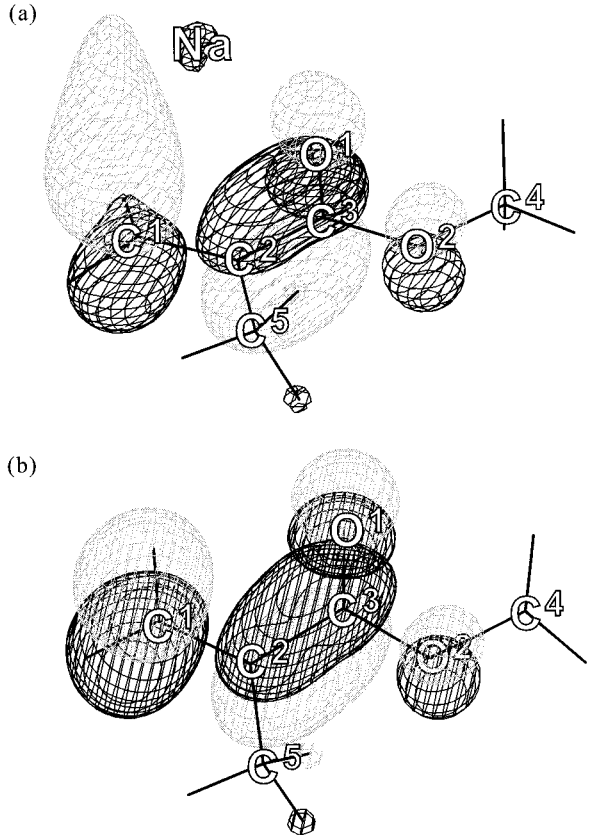

Figure 5. Contour surfaces of the square of atomic orbital coefficients of (a) SOMO for Na(*s-cis* MMA) (isomer II*a*) and (b) LUMO for free *s-cis* MMA.

structural changes can be explained by considering the electron density distribution in the singly occupied molecular orbital (SOMO) of isomer II*a*, as shown in Figure 5a. The electron density distribution in the SOMO of isomer II*a* resembles that of lowest unoccupied molecular orbital (LUMO) of free MMA (in Figure 5b), which has the antibonding nature of $C^1{=}C^2$ and $C^3{=}O^1$ and the bonding nature of $C^2{-}C^3$. Thus the changes of the bond lengths in Na(*s-cis* MMA) complex noted above are a result of valence-electron transfer of Na (3s) to MMA LUMO. Furthermore, electron transfer from the Na atom increases electron density at the C^2 atom in isomer II*a*. In general, electron density at the C^2 atom is important in the propagation of the anionic oligomerization reaction, because the reaction proceeds by nucleophilic attack by this atom to the C^1 atom of another MMA molecule. Present calculation reveals that the valence electron of the Na atom is mainly transferred to MMA in isomer II*a*; the natural charge on Na is +0.78. Therefore, it is expected that in the $Na(MMA)_3$ electron transfer from Na atom to $(MMA)_3$ takes place and induces the intracluster anionic oligomerization reaction.

D. Origin of the Dissociative Products. The fragment species assignable to the loss of ROH from $n = 3$ are observed in present mass spectra, as in the metal−acrylate system.[15] In our previous paper on metal−acrylate clusters,[15] we concluded that this fragment species was the complex containing the conjugate base of the cyclized β-ketoester produced by Dieckmann cyclization reaction. This dissociation reaction was found in the ion−molecule reaction study of the methyl acrylate system.[3] From the fact that methacrylate and acrylate have comparable reactivity for anionic polymerization as noted above, the fragment species from $n = 3$ in the present cluster can also be originated from Dieckmann cyclization at the trimeric oligomer (precursor of Dieckmann cyclization; **2**) (Scheme 2).

SCHEME 2

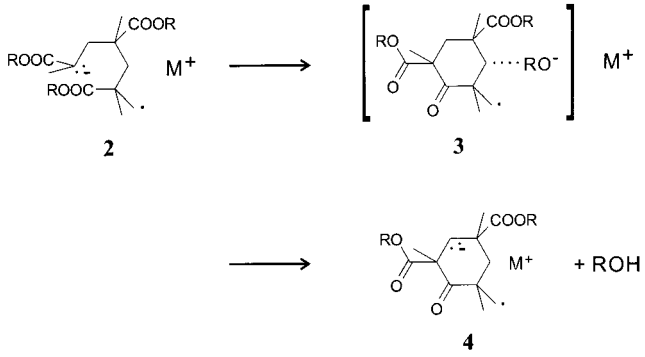

This precursor is produced by two successive 1,4-addition initiated by electron transfer from the metal atom and has a linear conformation. Dieckmann cyclization is an intramolecular condensation reaction with the loss of RO^- in an enolate anion of diester molecule. In the complex **3**, intracluster H^+ transfer to RO^- results in the corresponding carbanion of the cyclized β-ketoester (**4**). This reaction does not produce stable species in cluster sizes other than $n = 3$ because of their ring strain. Thus the observed fragment species from $n = 2$ is not expected to be produced by Dieckmann cyclization, and we need to consider other reaction processes to produce the fragment species from $n = 2$.

All possible intracluster reaction pathways induced by electron transfer from the metal atom to a methacrylate molecule in M(methacrylate)$_2$ are shown in Figure 6. Methacrylate anion has two reactive sites (α-carbon and carbonyl oxygen) for nucleophilic addition. These two sites can react with another monomer by 1,2- or 1,4-addition. 1,2-addition and the following dissociation products (**d** and **f**) starting from (i) and (ii), respectively, cannot explain a fragmentation reaction only from $n = 2$ or 3 because these dissociation reactions are possible in other cluster sizes. In the 1,4-addition product **e** from (ii), no intramolecular nucleophilic substitution reaction can be considered to dissociate ROH because there is no carbonyl carbon site attacked by nucleophilic site. Product **c** (Dieckmann cyclization product from **a**) has high ring strain as noted above, and thus the reaction is expected to be highly endothermic. Therefore, we conclude that the fragmentation from $n = 2$ is originated from lactonization reaction to produce **b**, which has lower ring strain than **c**. It is expected that the reaction barrier of lactonization (nucleophilic substitution by carbonyl oxygen) in diester is large, because no process to lose CH_3OH was observed in the reaction of RO^- with dimethyl glutarate in the gas-phase ion−molecule reaction study.[3] Moreover, this type of dissociation reaction from $n = 2$ was not observed in metal−acrylate study in our previous paper,[15] though the lactonization reaction has a possibility to proceed in M(acrylate)$_2$. Although the reason lactonization reaction occurs only in methacrylate case is not clear, it is possible that the nucleophilicity of carbonyl oxygen increases as a result of introducing the methyl group.

Next we discuss the difference on the yield of Dieckmann cyclization between the methacrylate and acrylate systems.[15] In the photoionization mass spectra of $M(MA)_n$ and $M(EA)_n$ (M = Na and K), the same magic number as the present study and the fragment ions assignable to the loss of ROH from $n = 3$ were also observed. However, the intensities of the fragment ions in the present study are c.a. 1/4 of those in the metal−acrylate systems. The relative intensity of fragment ion reflects the ratio between the yield of Dieckmann cyclization reaction (Scheme 2) and that of intracluster oligomerization (Scheme

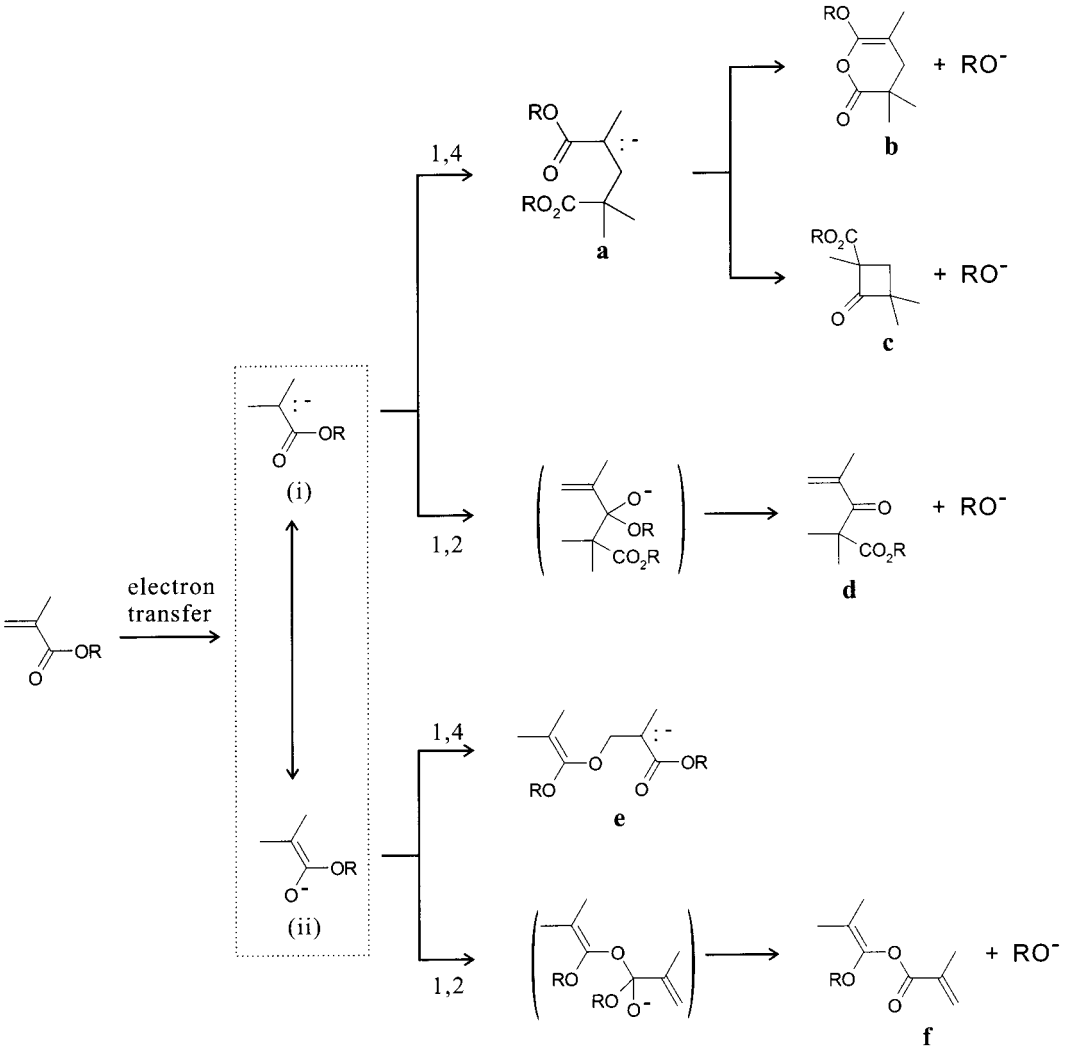

Figure 6. All possible intracluster reaction pathways induced by electron transfer from a metal atom to a methacrylate molecule in M(methacrylate)$_2$. (i) and (ii) are resonance structures of the enolate anion of a methacrylate molecule. All possible 1,2- and 1,4-addition reactions are shown. All reactions are depicted as intermolecular reactions, whereas these reactions take place in the M−methacrylate cluster.

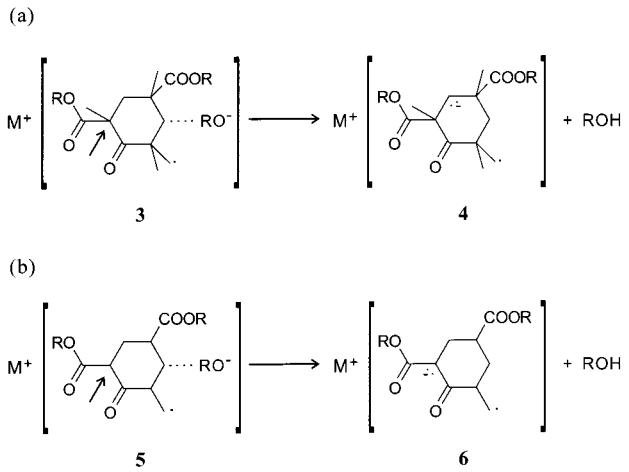

Figure 7. The reaction scheme of Dieckmann cyclization in (a) M(methacrylate)$_3$ and (b) M(acrylate)$_3$. Relevant carbon atoms are pointed by arrows, see text.

1). This difference can be explained by the relative stabilities of the products shown in Figure 7. The dissociative products (**4** and **6**) are produced by intracluster H^+ transfer from cyclized intermediates (**3** and **5**). The ability for H^+ donation of cyclic species is different between both cases. In the acrylate case, the hydrogen atom on the carbon pointed by an arrow in Figure 7 is easily transferred to RO^-, because the product of H^+ transfer (corresponding enolate anion) is stabilized by two carbonyl groups. However, there is no hydrogen atom on the carbon pointed by an arrow in methacrylate case, so that the product is less stable than that in acrylate case. Thus intracluster H^+ transfer is expected to be suppressed in Dieckmann cyclization for the methacrylate case.

E. Photoionization Mass Spectra of Alkali Metal−MMA−H_2O Clusters. In the typical mass spectra of M−methacrylate systems, small side peaks assignable to M(methacrylate)$_n$(H$_2$O)$_m$ are detected in larger cluster sizes (Figures 1 and 2). Therefore, we have measured the photoionization mass spectra of M−MMA (M = Li, Na, and K) system with intentional addition of water. Typical photoionization mass spectra of the Na−MMA−H_2O system with several different water mixing ratios are shown in Figure 8. In the mass spectrum with a trace amount of water impurity (Figure 8a), small side peaks assignable to Na^+-(MMA)$_n$(H$_2$O)$_m$ ($n \geq 6$) are detected along with the Na^+-(MMA)$_n$ ion series. Cluster ion intensities for $n \geq 6$, $m \geq 1$ clusters are enhanced with increasing water mixing ratio (Figure 8, parts b and c), whereas those for $n \leq 5$, $m \geq 1$ remain to be small. Even with a maximum water mixing ratio, $Na^+(H_2O)_n$ ion series are not observed, whereas these clusters are known to be produced by pickup-source apparatus.[29] This is probably because the water concentration is too small to produce the Na-

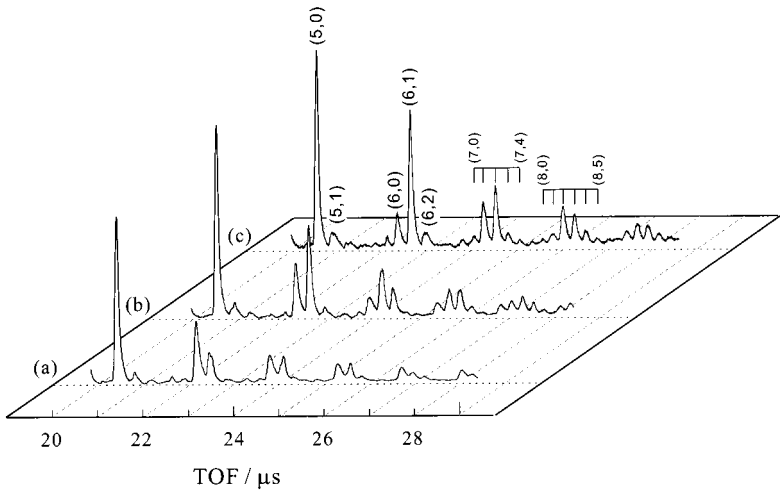

Figure 8. Photoionization TOF mass spectra of Na−MMA−H_2O system with several different water mixing ratios in the region of 20−29 μs. (a) Measured with a trace amount of water impurity. With increasing water mixing ratio, the mass spectra change from (a) → (b) → (c). (*n*,*m*) denotes the cluster ion of $Na^+(MMA)_n(H_2O)_m$.

$(H_2O)_n$ clusters even at maximum water concentration in the present condition. Similar change of water additivities to $M(MMA)_n$ clusters is also observed in Li− and K−methacrylate systems. We plot the fraction, $P_{n,m}$, of each ion intensity as a function of the number of MMA molecules n ($P_{n,m} = I_{n,m}/\sum_m I_{n,m}$; $I_{n,m}$: areal intensity of $M^+(MMA)_n(H_2O)_m$) for M = Li, Na, and K systems at the maximum water mixing ratio as shown in Figure 9. The fraction of the cluster containing water molecules abruptly increases at the threshold numbers $n_{th} = 5$ for Li, 6 for Na, and 7 for K systems, whereas the distribution of three-component clusters is expected to smoothly increase with n in general. This abrupt increase of water-containing clusters is also observed in the Na−EMA−H_2O system. This tendency was hardly observed in the acrylate system.[15]

The abrupt increase of the additivity of water molecules at a certain cluster size is considered to be related to the structures of hydrated clusters. We first consider the structures of M−MMA−H_2O clusters without any intracluster reactions, because the oligomerization does not necessarily proceed in the water-containing clusters. The metal−methacrylate clusters with the present study are produced at high-temperature condition as noted above. In this condition, the evaporation of molecules is expected after cluster formation. These evaporation processes induce breaking of intermolecular bonds with smaller binding energies. Therefore, we compare the binding energies of Na−MMA and Na−H_2O. The binding energy of Na−MMA is estimated to be 11.1 kcal/mol (Figure 4(II*a*)). As a result of the geometrical optimization for Na(H_2O), the binding energy is estimated to be 7.9 kcal/mol at the B3LYP/6-31+G(d) level. In addition, it was estimated to be 5.9 kcal/mol in a theoretical study for Na(H_2O) at the MP2/6-311+G(d) level.[38] Therefore, it is highly likely that H_2O molecules are dissociated more preferentially than MMA from M−MMA−H_2O clusters, and the first solvation shell in $M(MMA)_n(H_2O)_m$ clusters is composed of MMA molecules only. In the cluster where the first shell is closed, water molecules probably exist outside the first shell.

Next we consider the interaction of a H_2O molecule with MMA. MMA molecules are considered to have two hydrogen-bond acceptor sites—carbonyl oxygen and methoxy oxygen. These sites are also attractive in the interaction with an alkali metal atom. In both systems of MMA−H_2O and MMA−metal, carbonyl oxygen site is found to be more attractive than methoxy oxygen.[39] The metal−MMA cluster surfaces in which the first shell is filled have only weak attractive sites of methoxy oxygen because all carbonyl oxygen sites bind to a metal atom. Therefore, water molecules are considered to add to the MMA molecule of the second shell. MMA molecules coordinating outside the first shell are expected to have attractive sites of carbonyl oxygen, and can bind with H_2O molecules more preferentially than MMAs existing in the first solvation shell. From this consideration, the bond between H_2O and MMA in the first shell more easily dissociates in the cluster formation process than that between H_2O and MMA coordinating outside the first shell. Therefore we conclude that $n_{th} - 1$ is related to the number of MMA molecules filling the first solvation shell: 4, 5, and 6 MMA molecules are required to fill the first shell for Li, Na, and K systems, respectively. From these considerations, intracluster oligomerization reaction as in M−MMA clusters is expected to proceed in the present M−MMA−H_2O clusters, because the first solvation shell structures of the water-containing clusters may be approximated by those of the M−MMA systems.

Now we consider the interaction between the cyclized product and a metal atom or a water molecule. From the result of geometrical optimization (HF/6-31G) for the cyclized product (TMTMCHTCX), four conformational isomers were found in which each of three substituents ($-CO_2CH_3$) forms an axial or an equatorial conformation as shown in Figure 10. The most stable conformer among these isomers was found to have all axial conformation [(a,a,a)-TMTMCHTCX] (Figure 10d). In this (a,a,a) isomer, all substituents are in the same direction against the cyclohexane ring. The binding energy between the metal atom and the cyclized product is considered to be larger than that between the metal atom and a water molecule, because of the large dipole-induced dipole interaction in the former. Therefore only the cyclized product and some free MMA molecules are expected to be present in the first shell of the reaction product, as in the reactant system. In the M−(a,a,a) isomer complex, all carbonyl oxygen are presumed to orient to the central metal atom, and as a result, water molecules coordinate with weak attractive sites of the cyclized product from the outside of the first shell. Moreover, from the experimental results, the water molecules are expected to be more preferentially bound with MMA molecules existing outside the first shell also in the clusters containing reaction products, as in the reactant systems discussed above. Therefore, it is

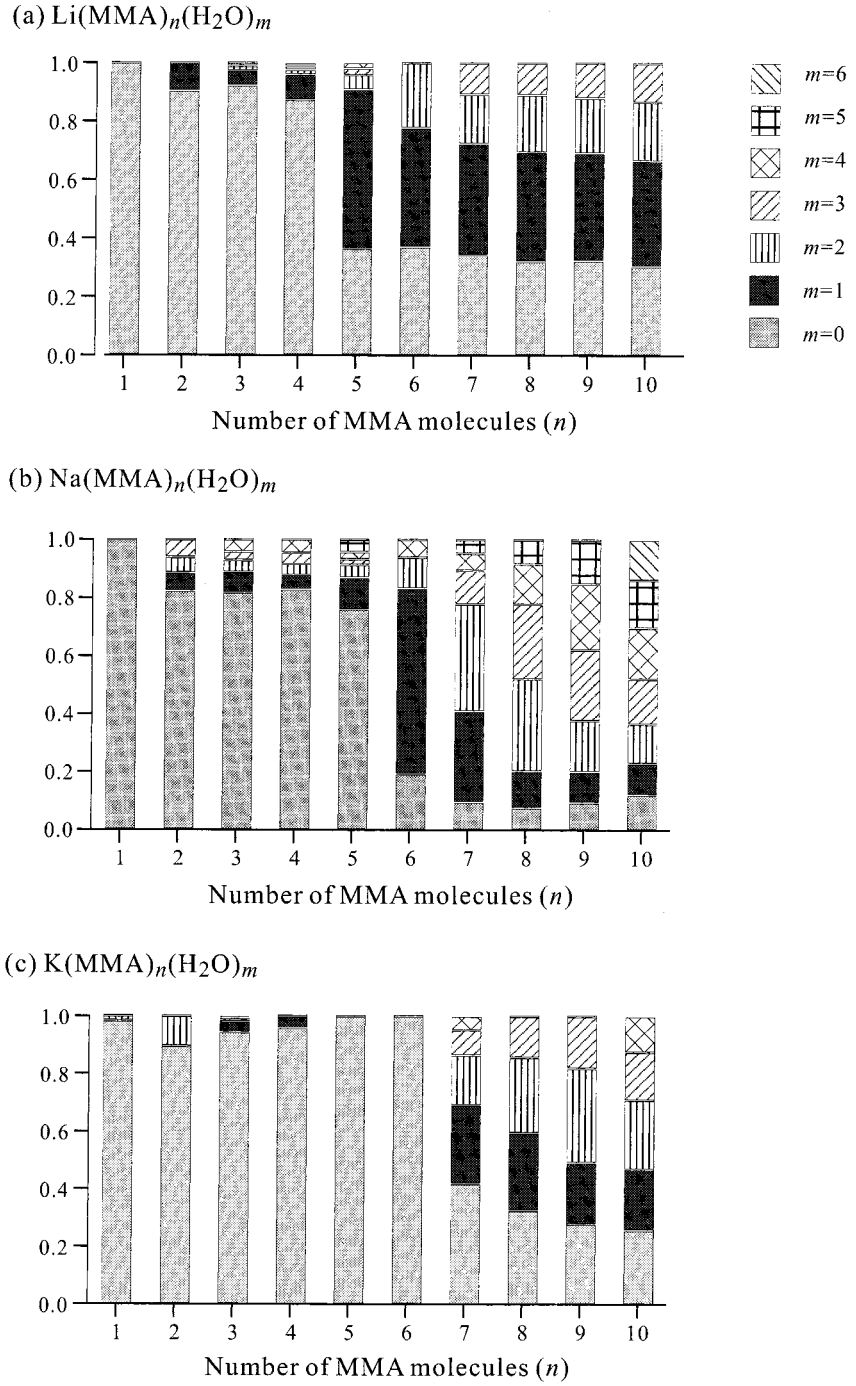

Figure 9. The fraction of each ion intensity as a function of the number of MMA molecules n, $P_{n,m} = I_{n,m}/\sum_m I_{n,m}$ ($I_{n,m}$: areal intensity of M^+-$(MMA)_n(H_2O)_m$), for (a) Li complex, (b) Na complex, and (c) K complex.

concluded that $n_{th} - 1$ corresponds to the number of MMA molecules filling the first solvation shell, including both the reacted and unreacted ones: 4, 5 and 6 MMA molecules are required to fill the first shell for Li, Na, and K systems, respectively. In other words, one cyclohexane derivative and one and two monomer(s) are directly bound to the metal atom in Li and Na systems, respectively. For the K system, two cyclohexane derivatives are expected to bond to the K atom, and therefore the magic number behavior at $n = 6$ specifically observed for K systems is consistent with this expectation. The appearance of these distinct threshold numbers n_{th} cannot be explained by considering other isomers than (a,a,a), because water molecules can coordinate with strongly attractive sites of the cyclized product in the first shell.

Next we examine the difference of the interaction distance between K and Na complexes, based on the geometrical optimization of K(MA) and Na(MA).[15] K(MA) complex has a similar structure with Na(MA) and Na(MMA) (see Figure 4). In the K(MA) complex, the bond lengths of K−C[1] and K−O[1] are 15% longer than in the Na complex. To calculate the distance between the metal atom and the cyclized product, we have optimized a structure of M−[trimethyl 1,3,5-cyclohexanetricarboxylate (TMCHTCX)] complex. TMCHTCX, which is the cyclized product in metal−acrylate system, has a similar binding site for a metal atom to the cyclized product in the methacrylate system, TMTMCHTCX. The distance between metal and carbonyl oxygen in the K−TMCHTCX complex is 13% longer than that in Na complex (Figure 11 a,b). These results suggest

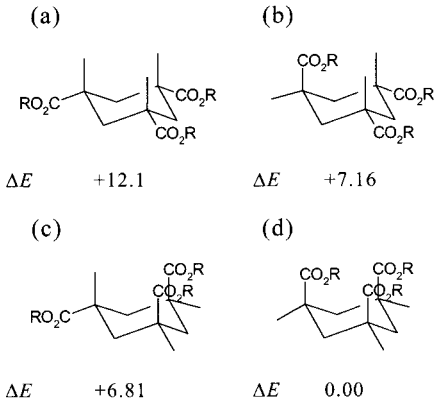

Figure 10. Structures of four conformational isomers of trimethyl 1,3,5-trimethylcyclohexane-1,3,5-tricarboxylate (TMTMCHTCX), (a) all equatorial conformation [(e,e,e)-TMTMCHTCX], (b) two equatorial and one axial [(a,e,e)-TMTMCHTCX], (c) one equatorial and two axial [(a,a,e)-TMTMCHTCX], and (d) all axial conformation [(a,a,a)-TMTMCHTCX] are shown. Energy differences (ΔE/kcalmol^{-1}) from the most stable isomer (a,a,a)-TMTMCHTCX are also shown.

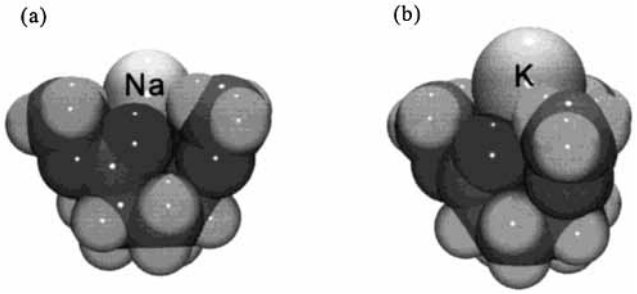

Figure 11. Optimized structures of (a) Na−[(a,a,a)-trimethyl 1,3,5-cyclohexanetricarboxylate (TMCHTCX)], (b) K−[(a,a,a)-TMCHTCX] at HF/6-31G level shown. The radius of each atomic sphere is proportional to the van der Waals radius. The structure of TMCHTCX is fixed in the geometrical optimization.

that a K atom can interact with more monomers than the Na atom. It is concluded that metal dependence of n_{th} can be explained by the difference of the interaction distance, on the assumption that the trimeric cyclization product has all axial conformation.

5. Conclusion

We have measured the photoionization mass spectra of clusters containing an alkali metal (M) and methacrylate molecules, M(methacrylate)$_n$. The intensity enhancement (magic number) at $n = 3$ is commonly observed for M = Li, Na, and K. The magic number at $n = 6$ is also observed for the K case. The fragment ion peaks assignable to a loss of ROH from $n = 2$ and 3 are also observed generally. The observed magic numbers at $n = 3$ and 6 can be attributed to cyclic trimer formation produced by anionic oligomerization induced by electron transfer from the metal atom. The fragment species can be ascribed to Dieckmann cyclization and lactonization reaction from $n = 3$ and 2, respectively. In the photoionization mass spectra of M−MMA−water clusters, M(MMA)$_n$(H$_2$O)$_m$, water containing clusters are found have certain threshold numbers of MMA molecules, n_{th}. The fraction of the cluster containing water molecules abruptly increases at $n_{th} = 5$ for Li, 6 for Na, and 7 for K systems. From the consideration of the stable structure of the clusters, the numbers, $n_{th} - 1$, can be attributed to the number of MMA molecules filling the first solvation shell. Therefore, it is suggested that one and two MMA molecules directly bind to the metal atom in Li or Na cases, respectively, in addition to one cyclohexane ring. Furthermore, the magic number at $n = 6$ observed in K−methacrylate clusters can be explained by a direct coordination of two cyclohexane derivatives to the K atom.

Acknowledgment. This work was partly supported by a Grant-in-Aid for Scientific Research from the Japanese Ministry of Education, Science, Sports and Culture. K. Ohshimo is supported by a Research Fellowship of the Japan Society for the Promotion of Science for Young Scientists. F.M. also acknowledges financial support from Mitsubishi Foundation.

References and Notes

(1) Hogen-Esh, T. E.; Smid, J. *Recent Advances in Anionic Polymerization*; Elsevier: New York, 1987.

(2) *Structure and Mechanism in Vinyl Polymerization*; Tsuruta, T., O'Driscoll, K. F., Eds.; Marcel Dekker: New York, 1969.

(3) McDonald, R. N.; Chowdhury, A. K. *J. Am. Chem. Soc.* **1983**, *105*, 2194.

(4) McDonald, R. N.; Chowdhury, A. K. *J. Am. Chem. Soc.* **1982**, *104*, 2675.

(5) Tsukuda, T.; Kondow, T. *Chem. Phys. Lett.* **1992**, *197*, 438.

(6) Tsukuda, T.; Kondow, T.; *J. Am. Chem. Soc.* **1994**, *116*, 9555.

(7) Tsukuda, T.; Kondow, T.; *J. Phys. Chem.* **1992**, *96*, 5671.

(8) Fukuda, Y.; Tsukuda, T.; Terasaki, A.; Kondow, T. *Chem. Phys. Lett.* **1996**, *260*, 423.

(9) Fukuda, Y.; Tsukuda, T.; Terasaki, A.; Kondow, T. *Chem. Phys. Lett.* **1995**, *242*, 121.

(10) Tsukuda, T.; Kondow, T.; Dessent, C. E. H.; Bailey, C. G.; Johnson, M. A.; Hendricks, J. H.; Lyapustina, S. A.; Bowen, K. H. *Chem. Phys. Lett.* **1997**, *269*, 17.

(11) Ichihashi, M.; Tsukuda, T.; Nonose, S.; Kondow, T. *J. Phys. Chem.* **1995**, *99*, 17354.

(12) Tsukuda, T.; Terasaki, A.; Kondow, T.; Scarton, M. G.; Dessent, C. E.; Bishea, G. A.; Johnson, M. A. *Chem. Phys. Lett.* **1993**, *201*, 351.

(13) Ohshimo, K.; Misaizu, F.; Ohno, K. *J. Phys. Chem. A* **2000**, *104*, 765.

(14) Ohshimo, K.; Tsunoyama, H.; Misaizu, F.; Ohno, K. *European Phys. J. D*, in press.

(15) Tsunoyama, H.; Ohshimo, K.; Misaizu, F.; Ohno, K. *J. Am. Chem. Soc.* **2001**, *123*, 683.

(16) El-Shall, M. S.; Yu, Z. *J. Am. Chem. Soc.* **1996**, *118*, 13058.

(17) Coolbaugh, M. T.; Whitney, S. G.; Vaidyanathan, G.; Garvey, J. F. *J. Phys. Chem.* **1992**, *96*, 9139.

(18) Coolbaugh, M. T.; Vaidyanathan, G.; Garvey, J. F. *Int. Rev. Phys. Chem.* **1994**, *13*, 1.

(19) Coolbaugh, M. T.; Vaidyanathan, G.; Peifer, W. R.; Garvey, J. F. *J. Phys. Chem.* **1991**, *95*, 8337.

(20) Lyktey, M. Y. M.; Rycroft, T.; Garvey, J. F. *J. Phys. Chem.* **1996**, *100*, 6427.

(21) Whitney, S. G.; Coolbaugh, M. T.; Vaidyanathan, G.; Garvey, J. F. *J. Phys. Chem.* **1991**, *95*, 9625.

(22) El-Shall, M. S.; Daly, G. M.; Yu, Z.; Meot-Ner (Mautner), M. *J. Am. Chem. Soc.* **1995**, *117*, 7744.

(23) El-Shall, M. S.; Marks, C. *J. Phys. Chem.* **1991**, *95*, 4932.

(24) Daly, G. M.; Pithawalla, Y. B.; Yu, Z.; El-Shall, M. S. *Chem. Phys. Lett.* **1995**, *237*, 97.

(25) Brodbelt, J. S.; Liou, C. C.; Maleknia, S.; Lin, T. Y.; Lagow, R. J. *J. Am. Chem. Soc.* **1993**, *115*, 11069.

(26) Wang, J.; Javahery, G.; Petrie, S.; Bohme, D. K. *J. Am. Chem. Soc.* **1992**, *114*, 9665.

(27) Pithawalla, Y. B.; Gao, J.; Yu, Z.; El-Shall, M. S. *Macromolecules* **1996**, *29*, 8558.

(28) Wiley: W. C.; McLaren, I. H. *Rev. Sci. Instrum.* **1955**, *26*, 1150.

(29) Schulz, C. P.; Haugstätter, R.; Tittes, H. U.; Hertel, I. V. *Phys. Rev. Lett.* **1986**, *57*, 1703.

(30) Schulz, C. P.; Haugstätter, R.; Tittes, H. U.; Hertel, I. V. *Z. Phys. D* **1988**, *10*, 279.

(31) Misaizu, F.; Sanekata, M.; Tsukamoto, K.; Fuke, K. *J. Phys. Chem.* **1992**, *96*, 8259.

(32) Frisch, M. J.; Trucks, G. W.; Schlegel, H. B.; Gill, P. M. W.; Johnson, B. G.; Robb, M. A.; Cheeseman, J. R.; Keith, T.; Petersson, G. A.; Montgomery, J. A.; Raghavachari, K.; Al-Laham, M. A.; Zakrzewski, V. G.; Ortiz, J. V.; Foresman, J. B.; Cioslowski, J.; Stefanov, B. B.; Nanayakkara, A.; Challacombe, M.; Peng, C. Y.; Ayalla, P. Y.; Chen, W.; Wong, M. W.; Andres, J. L.; Replogle, E. S.; Gomperts, R.; Martin, R. L.; Fox, D. J.; Binkley, J. S.; Defrees, D. J.; Baker, J.; Stewart, J. P.; Head-Gordon, M.; Gonzalez, C.; Pople, J. A. *Gaussian 94*, Revision E.2; Gaussian, Inc.: Pittsburgh, PA, 1995.

(33) Becke, A. D. *J. Chem. Phys.* **1993**, *98*, 5648.

(34) Tsuji, T.; Ito, H.; Takeuchi, H.; Konaka, S. *J. Mol. Struct.* **1999**, *475*, 55.

(35) Tsunoyama, H.; Ohshimo, K.; Misaizu, F.; Ohno, K. Unpublished results.

(36) Ohshimo, K.; Misaizu, F.; Ohno, K. To be submitted.

(37) Szwarc, M. Nature **1956**, *178*, 1168.

(38) Hashimoto, K.; Morokuma, K. *J. Am. Chem. Soc*. **1994**, *116*, 11436.

(39) For simplicity, we optimize the structure of MA−water 1:1 cluster instead of MMA−water at B3LYP/6-31+G(d) level. Two stationary points are found; the H atom of water binds to carbonyl oxygen (a) and that binds to methoxy oxygen (b). Binding energies with BSSE correction in both complexes are estimated to be 5.82 and 3.27 kcal/mol for (a) and (b), respectively. From the results of previous calculations (in ref 15), the binding energy between Na and carbonyl O was estimated to be 10.6 kcal/mol, and that between Na and methoxy O was 1.2 kcal/mol.